Cure kinetics and mechanisms of a tetraglycidyl-4,4′-diaminodiphenylmethane/diaminodiphenylsulphone epoxy resin using near i.r. spectroscopy

Nigel A. St John and Graeme A. George*
Chemistry Department, University of Queensland, Queensland 4072, Australia
(Received 22 March 1991; revised 9 August 1991; accepted 19 September 1991)

The cure of tetraglycidyl-4,4′-diaminodiphenylmethane with 27 wt% diaminodiphenylsulphone at 160°C was studied using near i.r. spectroscopy. The changes in concentrations of epoxy, hydroxyl, ether and primary, secondary and tertiary amine groups during cure were calculated and empirical reaction rate curves derived for the various functional groups involved. An autocatalytic reaction mechanism was observed for both the primary and the secondary amine group reaction with epoxide. The secondary amine–epoxy reaction showed a substitution effect and is affected by the changes in rheological properties of the resin during gelation and vitrification. Two separate epoxy–hydroxyl reactions are observed, as well as a cyclization reaction due to impurities.

(Keywords: near i.r. spectroscopy; chemo-rheology; cure kinetics; reaction mechanisms; epoxy resin)

INTRODUCTION

The wide application of amine cured epoxy resins and, in particular, the use of diaminodiphenylsulphone (DDS) cured tetraglycidyl-4,4′-diaminodiphenylmethane (TGDDM) epoxides in fabrication of high performance composite materials, has led to a high degree of research interest in the cure and properties of such resins. It is important to understand the mechanisms and kinetics of the various reactions involved in the cure of TGDDM/DDS resins as these factors directly control the final network structure and thus performance of the cured resins[1].

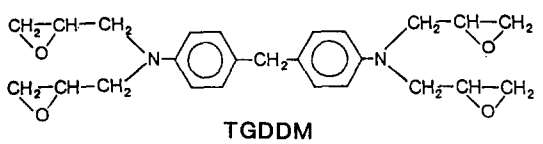

TGDDM

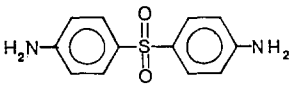

DDS

Several workers have used d.s.c. to investigate TGDDM/DDS cure kinetics[2,3] and empirical rate equations have been proposed. The applications of d.s.c. to the study of epoxy reactions have been reviewed by Barton[4]. The d.s.c. methods, however, only give a measure of overall reaction and require assumptions about the enthalpies of the individual reactions involved.

A radiochemical method[5] and g.p.c.[6] have been used to study amine–epoxy cure kinetics up to gelation and solid state ^{13}C n.m.r.[7,8] used to monitor the post-gelation TGDDM/DDS reaction. Morgan and Mones[1] carried out a detailed *FT*i.r. study of a TGDDM/DDS resin over the entire cure. All of these techniques required the cure reaction to be stopped to allow analysis with the resultant additional uncertainties. Considerable knowledge of the cure reactions involved and the resultant structural features of TGDDM/DDS resins has resulted from these investigations. However, a rigorous kinetic treatment has remained elusive.

To determine the kinetic parameters for the TGDDM/DDS cure reaction it is necessary to follow the three functional reactions presently accepted as describing the process of cure for most types of amine cured epoxy resins[9]. These are:

(1) Primary amine–epoxy addition

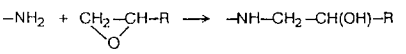

(2) Secondary amine–epoxy addition

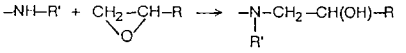

(3) Hydroxyl–epoxy (etherification)

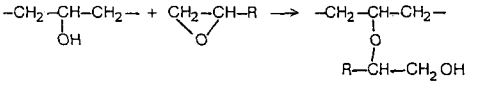

Other reactions are possible, such as an epoxy homopolymerization reaction, but have been considered of little significance at cure temperatures below 180°C for TGDDM/DDS[1]. The secondary amine–epoxy and etherification reactions can both occur intramolecularly

* To whom correspondence should be addressed

0032-3861/92/132679-10

to form ring structures instead of crosslinks[10]. Such cyclizations have been intimated from high resolution solid state ^{13}C n.m.r. studies[7,10] and may be very significant with respect to the mechanical properties of the resulting epoxy matrix. Whether there is any difference in the kinetics of the inter- and intramolecular reactions is as yet undetermined. Thus, they are treated as inseparable in most kinetic studies.

A remote technique using fibre optics coupled to a *FT*i.r. spectrometer configured for the near i.r. region has previously been developed to provide a real-time monitor of the TGDDM/DDS cure process[11]. In the near i.r. region (11 000–4000 cm^{-1}) the strongest absorption bands are due to the combination and overtones of fundamental CH, OH and NH vibrations. This is because of the large anharmonicity of vibrations involving the light hydrogen atom. Thus, the spectra are less complex than those obtained in the mid i.r. region. In addition, the bands are much weaker than for the fundamental vibrations allowing path lengths of 3–5 mm to be used for TGDDM/DDS mixtures rather than the experimentally more difficult and non-representative micrometre thick samples used for the mid i.r. range.

The information accessible using fibre optics was limited due to 'dead bands' in the spectra caused by the hydroxyl content of the silica fibre used, as well as the presence of cladding artifacts[11]. Thus, reliable data were only available for primary amine and hydroxyl groups. In the current work, direct transmission spectra are recorded using a quartz sample cell and a heating block mounted on the optical bench of the *FT*i.r. spectrometer. The higher quality spectra thus obtained have allowed a much more detailed spectral analysis to be carried out.

It has been possible to derive a measure of the changes in all the functional groups involved in the cure of TGDDM/DDS from the spectral data. This paper concentrates on the methodology used to obtain the different functional group data and the derived rate curves for the isothermal cure of 27 wt% DDS in TGDDM at 160°C. Kinetic analysis of the rate curves obtained is discussed in the light of proposed reaction mechanisms for the cure of TGDDM/DDS resins.

EXPERIMENTAL

Materials

The 27 wt% DDS formulation was prepared from the Ciba-Geigy epoxy resin MY721 which is ~92% TGDDM[7] and laboratory reagent grade DDS from Sigma Chemical Company. The sample was prepared by preheating the resin to 100°C, slowly adding a weighed portion of DDS and stirring until a clear mixture was obtained. The sample was then cooled and stored in a freezer until required.

Techniques

A Mattson Sirius *FT*i.r. spectrometer was used to record i.r. spectra. The instrument was configured to operate in the near i.r. from 11 000 to 4000 cm^{-1} using a 20 W tungsten quartz–halogen lamp, a quartz beam splitter and an indium antimonide (InSb) photovoltaic detector cooled to 77 K. To record data during isothermal cure a specially made heating block for use in the spectrometer was equilibrated at 160 ± 0.2°C. The resin sample was placed in a 3 mm diameter quartz tube which was then warmed in hot water prior to placement in the heating block. Spectra were recorded from the moment the tube was introduced into the heating block, although the sample took 2–3 min to reach the temperature of the heating block. Each spectrum was recorded automatically using a kinetics software routine and obtained from 32 scans at a resolution of 4 cm^{-1} which took 16 s to collect. Interference fringes due to the sample tube used were observed as a minor artifact and were removed by smoothing where it was considered necessary to enhance the evaluation of spectra.

The dynamic mechanical analysis (d.m.a.) of resin samples after the gel point was conducted on a Perkin–Elmer DMA7 instrument in 3 mm parallel plate configuration. The sample was held in a 5 mm diameter aluminium pan and heated at 160°C in the instrument furnace for 50 min before the probe was lowered and the isothermal (160°C) run started. This approach gives a qualitative measure of the changes in the resin during cure though the modulus values obtained are not precise. A frequency of 1 Hz and a constant 0.03% strain was used. Storage moduli and $\tan\delta$ were recorded as a function of cure time.

RESULTS AND DISCUSSION

Functional group analysis

The changes in the concentration of the amine, epoxy and hydroxyl groups were obtained from the near i.r. absorbance spectra at 160°C. Where required, deconvolution of the spectra were performed using a Fourier self-deconvolution routine to confirm the band position and determine likely spectral artifacts due to overlapping bands.

The accuracy of functional group concentrations derived using spectral data, assuming Beer's law, is generally good. However, the uncertainty increases significantly if several different experimental values are involved in the calculation as will be described, for example, for tertiary amine concentrations. This problem is addressed to some extent by collecting a large number of spectra over the course of the cure and digitally smoothing the concentration data before further numerical analysis. The concentration values obtained are estimated to be within 0.05 mol kg^{-1} in absolute terms, which is of relative significance only at low concentrations.

Primary amine. The combination band of the NH_2 stretching and bending vibrations at 5067 cm^{-1} is well resolved as seen in *Figure 1a*. The integrity of this peak as a measure of primary amine group concentration has been established previously[11]. The extinction coefficient for the band was calculated as 1.667 kg mol^{-1} cm^{-1} from the initial DDS concentration used. The peak was baseline corrected using points either side of the peak to enable peak height measurements to be made and the values obtained converted to primary amine group concentrations [PA] by using the extinction coefficient, so giving the curve shown in *Figure 1b*.

Secondary amine. The peak centred initially at 6678 cm^{-1} (*Figure 2a*) is a convolution of the symmetric and asymmetric stretching overtone bands for primary amine at 6685 and 6545 cm^{-1}, respectively, and the stretching overtone band for secondary amine at 6685 cm^{-1} (ref. 11). If the path length is constant, the

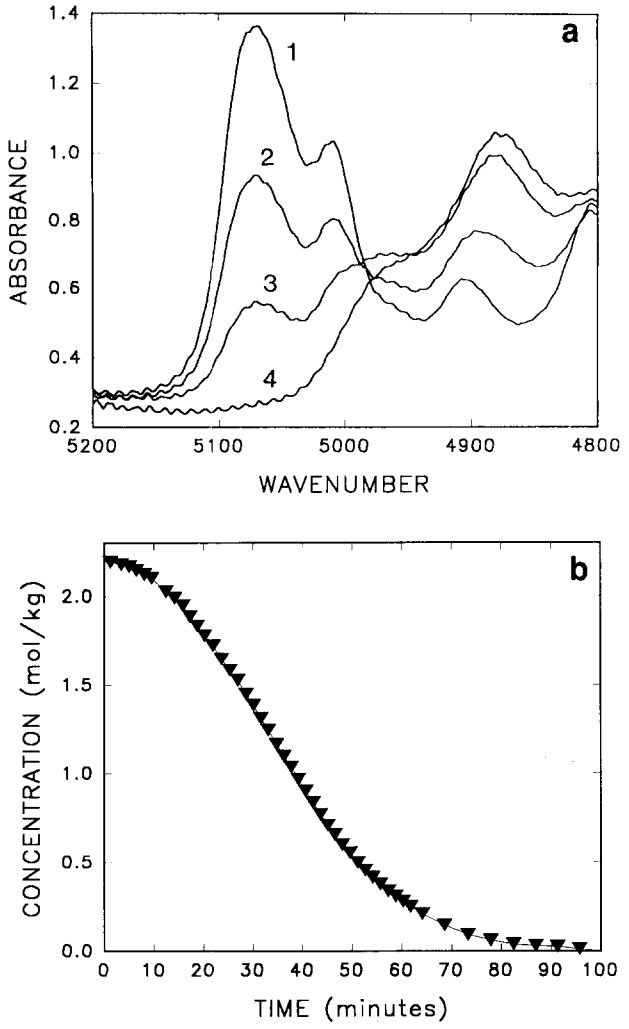

Figure 1 (a) Near i.r. spectra of primary amine combination band at (1) 0, (2) 25, (3) 45 and (4) 80 min cure at 160°C. (b) Plot of primary amine group concentration *versus* cure time

area of this peak (ΔA) can be described during the initial stages of cure by the relationship:

$$\Delta A = E_1[\mathrm{PA}]_t + E_2[\mathrm{SA}]_t \qquad (1)$$

where E_1 and E_2 are constants; and $[\mathrm{PA}]_t$ and $[\mathrm{SA}]_t$ are the primary and secondary amine group concentrations, respectively, at time t, and it is assumed that any secondary amine reaction is negligible over the first 10 min of cure. For different cure times one can insert values for $[\mathrm{PA}]_t$ and $[\mathrm{SA}]_t$ obtained from the primary amine data, conserving the total number of amine groups present. The set of simultaneous equations thus obtained can be solved for E_1 and E_2 giving the relationship for secondary amine concentration at any time t as:

$$[\mathrm{SA}]_t = (\Delta A - 29.9[\mathrm{PA}]_t)/18.0 \qquad (2)$$

The data shown in *Figure 2b* were calculated using this relationship; the [PA] values calculated using the peak at 5067 cm^{-1} and the area of the convoluted peak at 6678 cm^{-1}.

Tertiary amine. The concentrations of tertiary amine groups will increase during cure due to the further reaction of secondary amine groups with epoxy groups. The tertiary amine group cannot be seen in the near i.r. spectrum, so its concentration is determined by a mass balance between the secondary amine concentration calculated from the consumption of primary amine and that measured from spectral data using the relationship:

$$[\mathrm{TA}]_t = [\mathrm{PA}]_0 - [\mathrm{PA}]_t - [\mathrm{SA}]_t \qquad (3)$$

where $[\mathrm{PA}]_0$ is the initial concentration of primary amine and $[\mathrm{TA}]_t$ is the concentration of tertiary amine groups produced by reaction of secondary amines at any time t. The concentration during cure calculated from this relationship is shown in *Figure 2b*.

Hydroxyl. A value for the total hydroxyl group concentration $[\mathrm{OH}]_t$ was obtained (*Figure 3b*) from the amine group reaction data by assuming the epoxy–amine reaction is the only source of increase in the hydroxyl group concentration at the cure temperature used[1]. As discussed below, the etherification reactions produce no net increase in hydroxyl group concentration. It is necessary to calculate such a hydroxyl value as the spectral information obtainable for hydroxyl groups in the near i.r. is complicated by the significant effect of hydrogen bonding on both the shape and position of the hydroxyl overtone band.

$$[\mathrm{OH}]_t = [\mathrm{PA}]_0 - [\mathrm{PA}]_t + [\mathrm{TA}]_t \qquad (4)$$

The peak at 7000 cm^{-1} (*Figure 3a*) is assigned as the

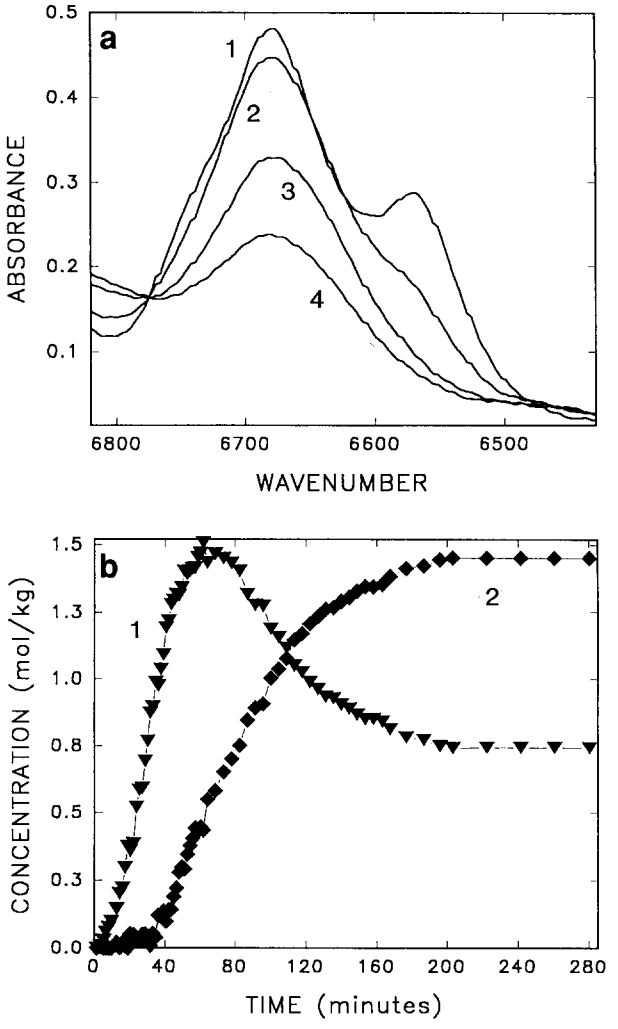

Figure 2 (a) Near i.r. smoothed spectra of amine overtone peaks at (1) 0, (2) 40, (3) 80 and (4) 200 min cure at 160°C. (b) Plot of (1) secondary and (2) tertiary amine group concentration *versus* cure time

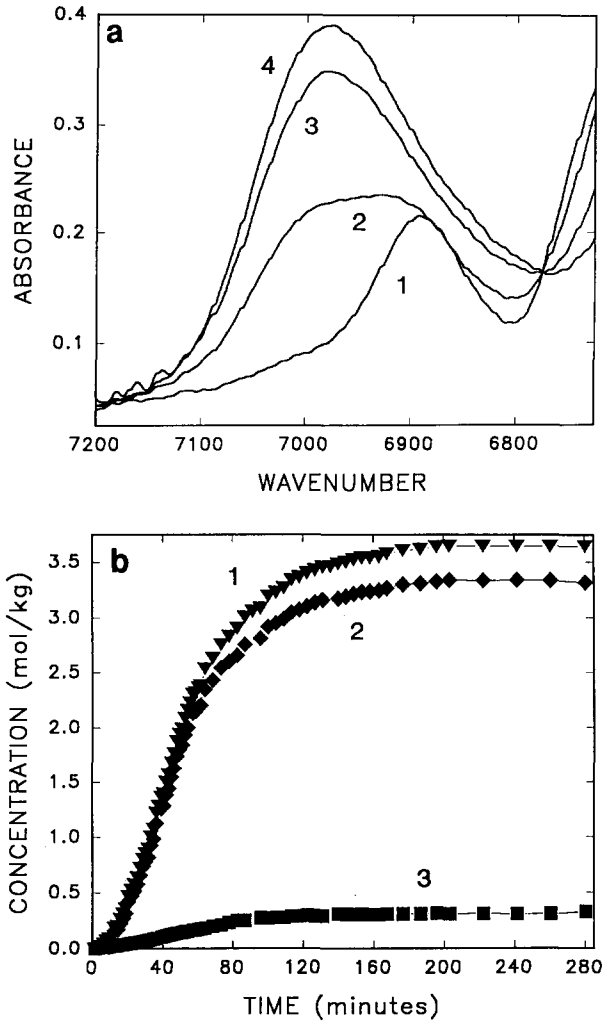

Figure 3 (a) Near i.r. smoothed spectra of hydroxyl overtone band at (1) 0, (2) 40, (3) 80 and (4) 200 min cure at 160°C. (b) Plot of (1) total, (2) hydrogen-bonded and (3) free hydroxyl group concentration *versus* cure time

OH stretching overtone band and represents only the non-hydrogen-bonded species[12]. The hydrogen-bonded species are seen as a very broad, weak band at lower wavenumber. To estimate the degree of hydrogen bonding in the network the extinction coefficient for the OH overtone peak of 2-propanol[13] was used to convert the height of the 7000 cm^{-1} peak to a concentration value. The free hydroxyl group concentration curve thus obtained (*Figure 3b*) shows that on average only 8% of the total hydroxyl present is not hydrogen bonded at 160°C.

Epoxy. To follow the conversion of epoxy groups several different bands in the near i.r. have been used[11]. The overtone of the epoxy CH combination band at 8627 cm^{-1} is not very intense and is overlapped by the overtone of the OH combination band at 8212 cm^{-1} (ref. 11). To obtain a better measure of epoxy group concentration Fourier self-deconvolution of the CH stretching overtone peaks was performed (*Figure 4a*). The peak resolved at 6060 cm^{-1} is assigned as the overtone of the CH stretching vibration of the terminal epoxy group[14].

Studies of synthetic spectra[15] have shown that there is no significant loss of quantitative information using Fourier self-deconvolution if care is taken in choosing the apodization function and enhancement factor. To confirm this in our case the area of the peak obtained by self-deconvolution was compared over the early stages of cure with the decrease in the area of the epoxy overtone peak at 8627 cm^{-1}, obtained by subtracting each spectrum

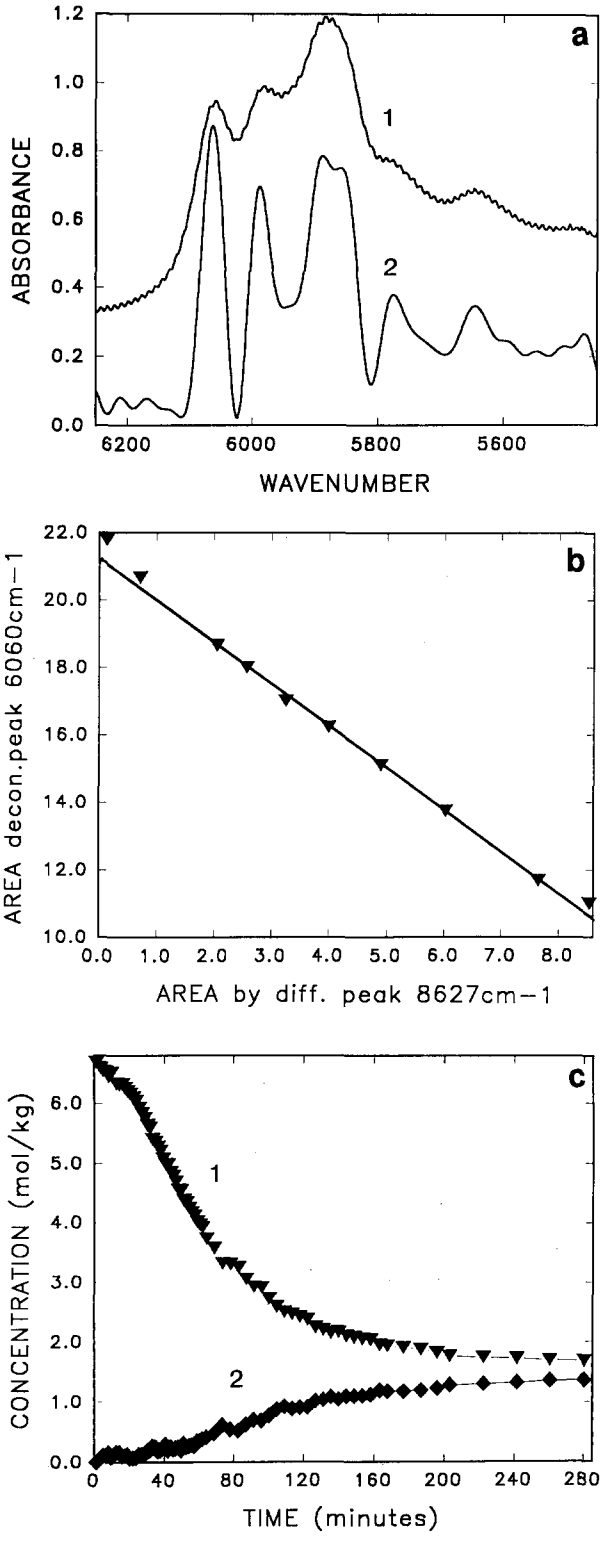

Figure 4 (a) Near i.r. spectrum of CH overtone region for uncured resin (1) before and (2) after Fourier self-deconvolution. (b) Plot of area of deconvoluted peak at 6060 cm^{-1} *versus* area of peak by difference at 8627 cm^{-1}. (c) Plot of (1) epoxy and (2) 'excess' epoxy group concentration *versus* cure time

from the spectrum collected at the start of cure. A linear relationship was observed (*Figure 4b*) thus validating the use of Fourier self-deconvoluted areas.

To convert peak area to epoxy group concentration [EP] the change in peak area was compared with the change in amine group concentrations to obtain an appropriate factor assuming the amine addition reaction is the only one involving epoxy groups in the early stages of cure. The results are plotted in *Figure 4c*. Since ring-opening of the epoxide will produce a hydroxyl group there should be an equal concentration of hydroxyl groups formed for epoxy groups consumed. This is not observed and there is an 'excess' epoxy reaction that is not accounted for by reaction with primary and secondary amine groups given by:

$$\Delta[EP]_{XS} = [EP]_0 - [EP]_t - [OH]_t \qquad (5)$$

This is also plotted in *Figure 4c* and most likely represents the epoxy groups consumed via etherification reactions.

Rate curves and kinetic analysis

Data manipulation. Empirical rate curves were generated for the various reaction species by first using a cubic spline function to create equispaced functional group data in the x-ordinate (i.e. time) to allow the various numerical analyses to be performed. These curves were smoothed with a five-point weighted smoothing function using the minimum number of iterations to obtain a smooth curve. Visual inspection of each curve against the original after each step was used to ensure faithful transformations. The empirical rate curves were then generated by applying a five-point derivative function to the smoothed curves. This procedure ensured that the instantaneous reaction rates obtained from the concentration profiles were not affected by single data point error.

The rate curves based on various kinetic models were calculated using the functional group concentration data. The rate constants were then determined by finding a 'best fit' with the empirical rate curves by iteration. It is difficult to attach a confidence level to the rate constants thus obtained. However, the greatest uncertainty is expected to be in the calculated rate curves, due to the error associated with the empirical concentration data used. This is estimated to translate into an uncertainty in the rate constants obtained of the order of 10%.

Primary amine reaction. The empirical rate curve for the primary amine reaction obtained by analysing the concentration–time data of *Figure 1b* is shown in *Figure 5*. The curve is clearly autocatalytic in nature[16] and the best kinetic fit of the proposed mechanisms is that involving autocatalysis by the hydroxyl groups formed in the course of the cure. A simple autocatalytic rate curve using a rate contant of 6.75×10^{-3} kg^2 mol^{-2} min^{-1} is also shown in *Figure 5* and it is seen that while this is able to describe the empirical rate curve over much of the reaction, significant deviation is observed at short cure time. The residual rate curve was obtained by subtracting the calculated autocatalytic curve from the measured rate curve (*Figure 5*). This residual reaction was found to be reproducible and is most likely due to either the amine catalysed epoxy–amine reaction or catalysis by an initial concentration of an impurity such as the original hydroxyl groups from the synthesis of the resin[7]. This will be discussed further later. The following empirical kinetic expression is accordingly derived where the first term represents the autocatalysis and the second term the rapid, initial reaction in which k and X are yet to be determined.

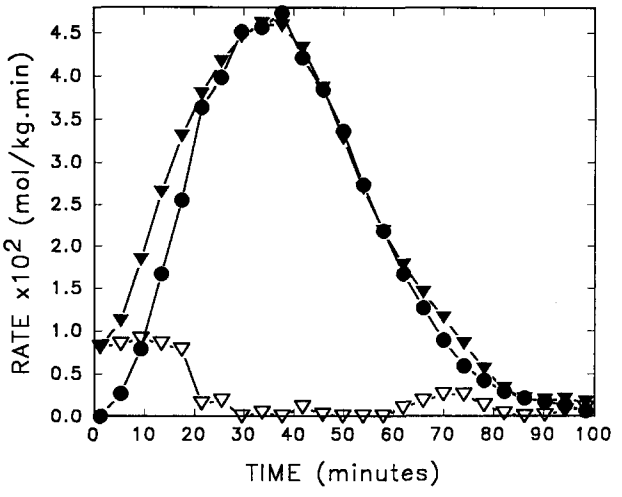

Figure 5 Plot of the primary amine group consumption empirical reaction rate $-d[PA]/dt$ (▼), calculated reaction rate using $6.75 \times 10^{-3}[PA][OH][EP]$ (●) and residual reaction rate after subtracting the calculated rate from the empirical rate (▽) *versus* cure time

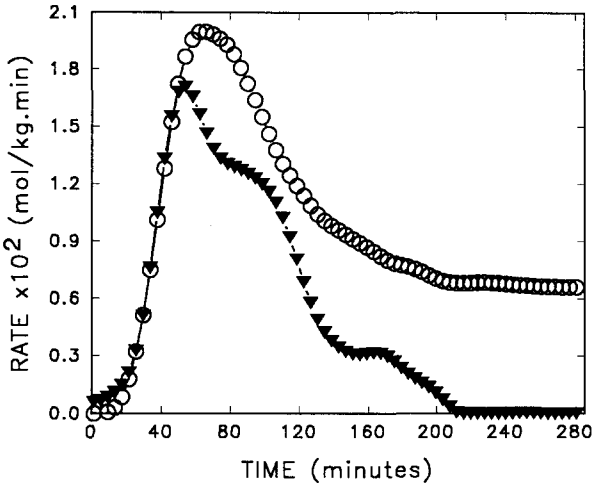

Figure 6 Plot of the tertiary amine group production empirical reaction rate $d[TA]/dt$ (▼) and the calculated reaction rate using $1.45 \times 10^{-3}[SA][OH][EP]$ (○) *versus* cure time

$$-d[PA]/dt = 6.75 \times 10^{-3}[PA][EP][OH] + k[PA][EP][X] \qquad (6)$$

Secondary amine reaction. To study the reaction of the secondary amine groups, the empirical rate curve for tertiary amine production was generated. This avoided the complication of the competition kinetics between the creation of secondary amine groups from the primary amine–epoxy reaction and their consumption by the (slower) amine–epoxy reaction. The curve thus obtained (*Figure 6*) is matched well by the curve generated using kinetics based on autocatalysis by hydroxyl groups, using a rate constant of 1.45×10^{-3} kg^2 mol^{-2} min^{-1}, though only over the first 50 min of cure. The failure of the predicted rate at 50 min cure corresponds to the onset of gelation of the resin, i.e. a sharp increase in viscosity[3].

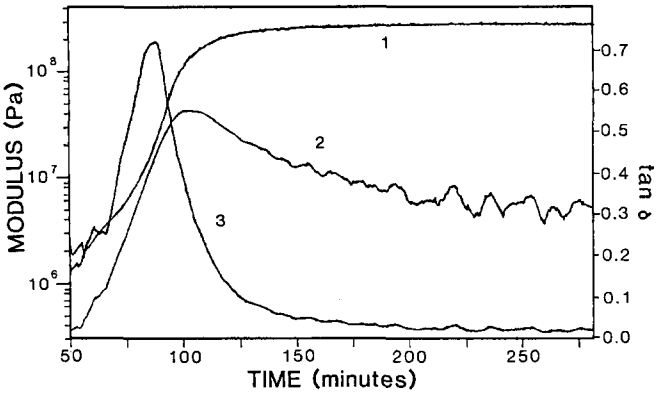

Figure 7 Plot of (1) storage modulus G', (2) loss modulus G'' and (3) tan δ *versus* cure time at 160°C starting from gelation

The secondary amine–epoxy reaction is thus very sensitive to diffusion control which is clearly seen in the sharp drop in rate at gelation. The rate equation for the secondary amine reaction up to gelation is then given by:

$$d[TA]/dt = -d[PA]/dt - d[SA]/dt$$
$$= 1.45 \times 10^{-3}[SA][EP][OH] \quad (7)$$

To better understand the post-gelation rate curve, changes in the dynamic mechanical properties of the resin during the isothermal cure at 160°C were measured. *Figure 7* shows the changes in storage modulus (G'), loss modulus (G'') and tan δ during the post-gelation curing.

One sees an increase in both G' and G'' after gelation which is indicative of the increasing number of chemical bonds present to resist deformation as well as additional paths for energy dissipation which are available. The observed rate curve reflects this with diffusion effects on the reaction rate increasing, but stabilizing, for the secondary amine reaction in this region. At around 85 min cure a peak occurs in the tan δ curve which can be interpreted as the point where large chain motions start to be 'frozen out' at the cure temperature. This is due to the increasing number of crosslinks which restrict the motion of chains. This point in the cure may be termed the onset of vitrification within the gel network[17]. This is evident as an inflection in the rate curve at 85 min cure. A rapid drop in reaction rate sets in after some 100 min which is the point where G'' peaks and starts to decline signifying the dominance of the 'freezing out' of chain movements over the creation of additional paths for energy dissipation. The drop in rate continues till around 150 min cure, where G' is seen to be unchanging, and vitrification is complete. At 150 min cure it is thus expected that the glass transition temperature of the resin equals the cure temperature, i.e. 160°C[3].

Following vitrification the secondary amine groups continue to react, though very slowly, producing more crosslinks and so decreasing G'' and the reaction rate. After 210 min cure the secondary amine–epoxy reaction is totally arrested, even though 34% of the secondary amine groups produced from the primary amine–epoxy are still unreacted.

Epoxy reaction and etherification. The empirical rate curve for the epoxy group reaction (*Figure 8a*) shows similar behaviour to that for the secondary amine reaction with an inflection in the curve at around 85 min cure, previously described as the onset of vitrification. A change in the curve is also seen after 150 min cure, as expected when vitrification is complete, with the rate then reducing slowly. The bump in the curve around 200 min cure is probably an artifact due to the limited experimental data collected and the small changes occurring during the final stages of cure.

Of particular interest is the empirical rate curve (*Figure 8a*) of the remaining epoxy reaction after subtracting the reaction of epoxy groups with primary and secondary amines (*Figure 4c*). It is evident from the complexity of this curve that more than one mechanism is involved. The 'best fit' obtained of the curve up to gelation, based on previously proposed mechanisms[18], is shown in *Figure 8b*. It was necessary to invoke two mechanisms for etherification as shown. The first (curve 2) is an apparently uncatalysed reaction between epoxide and hydroxyl groups, though catalysis by tertiary amine groups in TGDDM is a possibility as the concentration is constant during the cure. The second (curve 3) involves the reaction of epoxy and hydroxyl groups catalysed by the tertiary amine groups produced by reaction of secondary amine and epoxy groups, as proposed by Cole *et al.*[18]. After subtracting the two kinetic curves derived

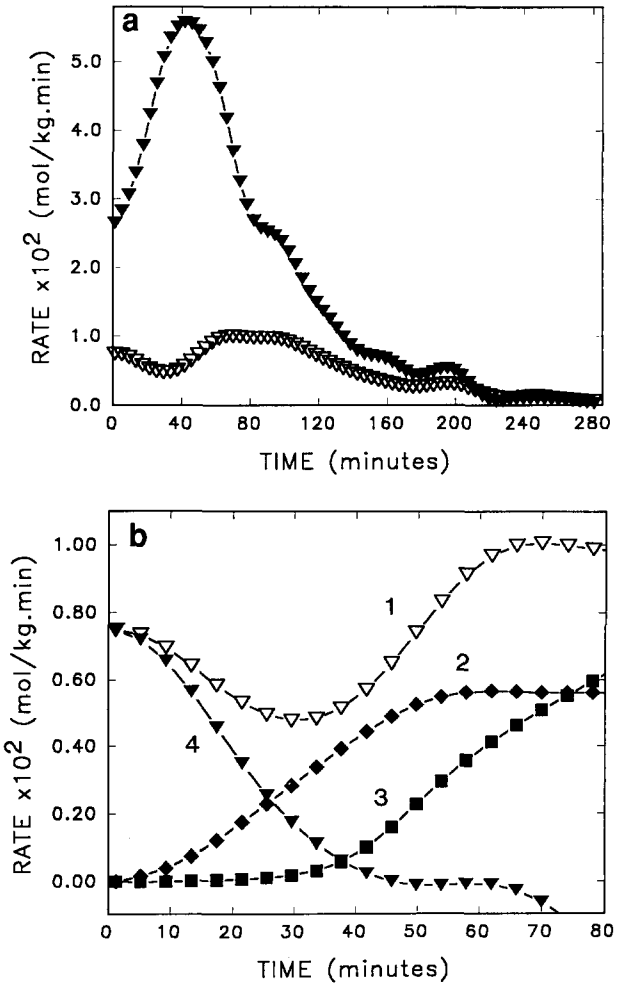

Figure 8 (a) Plot of the epoxy group consumption empirical reaction rate $-d[EP]/dt$ (▼) and the empirical 'excess' epoxy reaction rate (▽) *versus* cure time. (b) Plot of (1) empirical 'excess' epoxy reaction rate, (2) calculated etherification reaction rate using $6.0 \times 10^{-7}[EP][OH]$, (3) calculated etherification reaction rate using $9.0 \times 10^{-4}[EP][OH][TA]$ and (4) empirical epoxy reaction rate remaining after subtracting curves (2) and (3) from (1) *versus* cure time

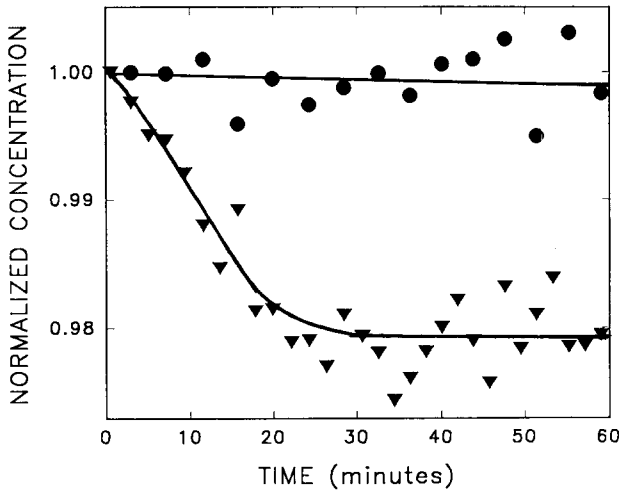

Figure 9 Plot of normalized epoxy group concentration for neat MY721 (▼) and LC purified TGDDM (●) *versus* time at 160°C

from these two mechanisms, we obtain a declining rate curve (curve 4) for the remaining epoxy reaction (*Figure 8b*).

One explanation for the initial extra epoxy reaction (curve 4) is the involvement of some impurity in the resin. To investigate this further the behaviour of the neat TGDDM resin used (MY721) at 160°C was studied. The change in the epoxy band was monitored as before and an initial decrease, levelling off after 30 min, was in fact observed (*Figure 9*). A similar study of a resin sample purified by liquid chromatography showed no detectable change in the epoxy band (*Figure 9*).

Recent studies of the impurities in TGDDM resins[19] have shown that *N,N,N'*-triglycidyl-4,4'-diaminodiphenylmethane, *N,N,N'*-triglycidyl-*N'*-(2-hydroxy-3-chloropropyl)-4,4'-diaminodiphenylmethane (I), 1,2,3,4-tetrahydro-3-hydroquinoline (II), dimers and higher oligomers are the major by-products in the synthesis of TGDDM. To identify which, if any, of these impurities was involved in the observed phenomenon the difference in the i.r. spectrum after heating the resin at 160°C for 1 h was recorded (*Figure 10*). A decrease in the aromatic CH bending vibrations at 1608, 1513 and 800 cm^{-1} was observed along with a decrease in a peak at 670 cm^{-1} which we have assigned as the C–Cl vibration[20]. These assignments and changes in band intensity on cure suggest that it is the chlorohydrin impurity (I) that is reacting in a cyclization reaction to form 1,2,3,4-tetrahydro-3-hydroquinoline (II) compounds.

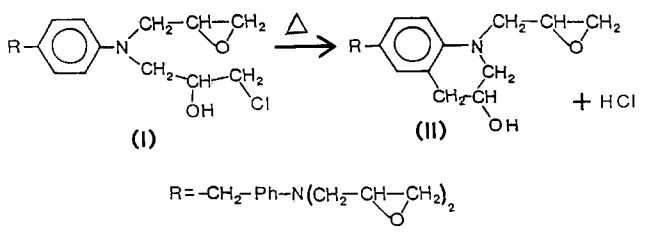

A similar reaction has been reported[21] for the thermal dehydrochlorination of *N*-methyl-*N*-(2-hydroxy-3-chloropropyl)aniline to give a cyclic product at 180–220°C. Recently Podzimek *et al.*[22] described a kinetic study of the intramolecular cyclization of *N,N*-bis(2-hydroxy-3-chloropropyl)aniline at temperatures of 70–115°C. An extrapolation of these results to 160°C gives a reaction rate that is faster than, though of the same order of magnitude as the additional reaction observed for MY721. Attias *et al.*[10] have also reported observing such a cyclic product in n.m.r. studies of TGDDM/DDS resins during cure.

It is worth noting that the CH stretching vibration for $-CH_2-Cl$ is reported[20] at ~3050 cm^{-1} which makes it quite likely that the overtone of this band is degenerate with the CH overtone band at 6060 cm^{-1} for terminal epoxy groups. It is likely then that the initial extra epoxy reaction measured is in fact, at least partially, not an epoxy reaction at all but instead a reaction of chlorohydrin groups. In addition, the hydrogen chloride produced by such a reaction could catalyse the epoxy ring-opening reaction explaining some additional reaction in the early stages of cure.

If one disregards impurity effects we obtain the following rate equation for etherification up to gelation:

$$d[ET]/dt = 6.0 \times 10^{-7}[EP][OH] + 9.0 \times 10^{-4}[EP][OH][TA] \quad (8)$$

and for the overall epoxy reaction up to gelation:

$$-d[EP]/dt = (6.75 \times 10^{-3}[PA] + 1.45 \times 10^{-3}[SA] + 9.0 \times 10^{-4}[TA] + 6.0 \times 10^{-7})[EP][OH] \quad (9)$$

Cure mechanisms

The pre-gelation rate curves clearly show that the dominant mechanism for both the primary and secondary amine groups reaction with epoxide is one involving catalysis by a hydroxyl group. This is consistent with previous studies[23] which found that the amine–epoxy reaction can only proceed by a catalysed mechanism. Hagnauer *et al.*[6] found a third-order rate expression that was first order with respect to TGDDM (epoxy) and second order with respect to DDS (primary amine) in a study of the cure of a high purity TGDDM/DDS resin. However, this appears to have been determined from initial rates of reaction and so is consistent with the finding that if no hydroxyl groups are present, in this case at the start of cure, then the reaction will be catalysed

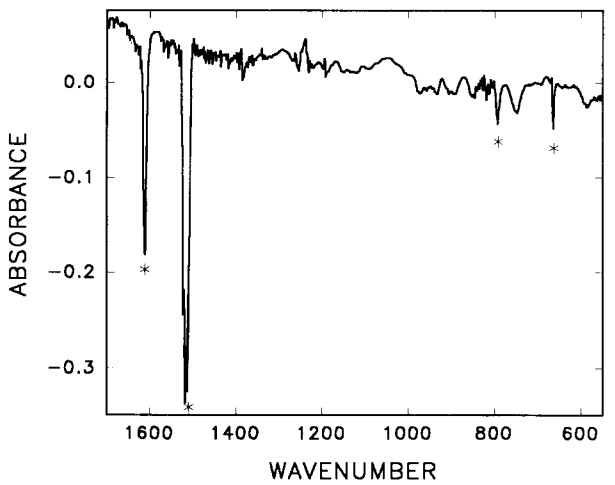

Figure 10 Difference of *FT*i.r. spectrum obtained 'after' minus 'before' heating neat MY721 at 160°C for 1 h. Changes in peaks marked with an asterisk are discussed in the text

by the amine groups themselves, though less efficiently than hydroxyl groups[23]. The early primary amine reaction not accounted for by the autocatalytic mechanism may well be due to such a mechanism. Once hydroxyl groups are generated in the reaction the rate expression describing the reaction would change to first order with respect to epoxy, primary amine and hydroxyl concentrations as observed. In fact Hagnauer *et al.* went on to show that autocatalytic behaviour was indeed observed with their d.s.c. data[6].

The other feature of the amine reaction kinetics is the substantial substitution effect observed for the secondary amine–epoxy reaction. Previous investigations[18] have been inconclusive on this point as it has not been possible before to measure independently the secondary amine–epoxy reaction for TGDDM/DDS. The ratio of rate constants for secondary and primary amine reactions with epoxide, often quoted as k_2/k_1, is expected to be 0.5 if the hydrogen on the secondary amine nitrogen has equal reactivity to that of each of the two hydrogens on the primary amine group. Our results give a ratio of 0.215 showing that the secondary amine group is less than half as reactive as the primary amine hydrogens. This could arise from the steric hindrance caused by the substitution on the nitrogen atom. The significant contribution of etherification reactions observed for the cure of the TGDDM/DDS resin, as well as the chemo-rheological effects discussed later, may explain the problems in the past in obtaining agreement on the existence of a substitution effect on the reactivity of secondary amine groups in this and similar systems[23].

The functional group data illustrate the difficulty in obtaining total cure of a TGDDM/DDS resin, as a high concentration of secondary amine groups (34% of that produced) is still present after 4 h cure at 160°C. At higher temperatures (180–250°C) the remaining epoxy groups would be consumed through a variety of reactions, including thermal decomposition, but the secondary amine groups left would remain essentially unreacted[1]. The high level of secondary amine groups present in a cured epoxy matrix can adversely affect its environmental performance[24] and mechanical properties[3]. Thus, being able to describe the cure process in sufficient detail to allow the secondary amine–epoxy reaction to be maximized is very advantageous.

It is evident from the functional group data (*Figures 2b* and *4c*) that the number of ether links created during curing is similar to the number of secondary amine groups reacted (trivalent crosslink nodes). The fact that the etherification reaction is slower than the secondary amine–epoxy reaction is countered by the epoxy to amine stoichiometry (1.5:1) used. Attias *et al.*[10] claim that the majority of ether groups are involved in cyclic moieties and therefore contribute little to the overall network structure.

The etherification reaction is interesting in that there are two apparent mechanisms involved with the cure of TGDDM/DDS. The first involves a rate-determining step consisting of an uncatalysed reaction between epoxy and hydroxyl groups, probably in a similar way to the acid-catalysed epoxy reaction mechanism[25] as shown in *Scheme 1*. The preferred product in such a case is likely to be a primary alcohol[25].

The second mechanism involves catalysis by the tertiary amine groups produced on the former DDS units by the epoxy–amine reactions. Rozenberg describes a

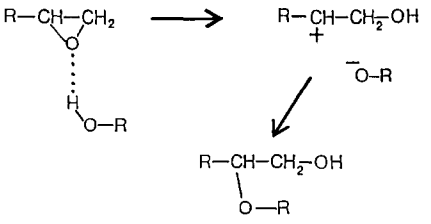

Scheme 1

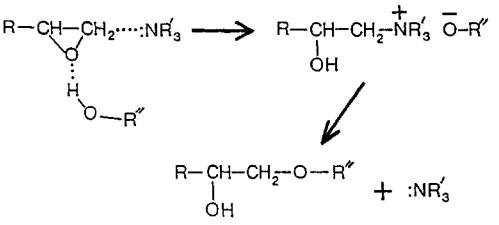

Scheme 2

mechanism for tertiary amine catalysis of epoxy group reactions[23] as shown in *Scheme 2*.

If this mechanism is correct one might also expect the tertiary amine groups in TGDDM to catalyse the epoxy–hydroxyl reaction. The previous 'uncatalysed' reaction may in fact represent such a situation as discussed earlier. However, if the kinetics are assessed for this case the TGDDM tertiary amines show a catalytic activity of only 10% of that observed for the tertiary amines produced during cure. The reason for the absence or limitation of catalysis by the TGDDM tertiary amines may lie in the fact that for TGDDM the nitrogen lone electron pair is unable to interact with an epoxy group attached to the same nitrogen atom due to bond constraints, whereas the epoxy group can easily associate with a nitrogen atom on a DDS unit attached by reaction. This has been borne out by inspection of molecular models of the structures involved. Intramolecular reaction would be favoured in this case which supports the findings of solid state ^{13}C n.m.r. studies of cured TGDDM/DDS that cyclic products are dominant[8,10].

Another consequence of the two etherification mechanisms is that while an uncatalysed reaction favours primary alcohols as products, the tertiary amine catalysed reaction favours a secondary alcohol product. Grenier-Loustalot *et al.*[26] report the appearance of primary alcohol groups during cure of a TGDDM/DDS resin with a slight decline in secondary alcohol group concentration over a similar period which is consistent with the existence of an uncatalysed reaction mechanism.

Chemo-rheology

The rate curves derived from experimental data also describe the chemo-rheological effects during the cure of TGDDM/DDS; that is, the correlation between chemical reactivities and rheological properties. For primary amine the reaction with epoxide appears to be unaffected by the rise in viscosity during gelation. This could be due to the fact that primary amine groups must be on the end of chains and the majority would be found in the sol fraction during gelation. Thus the primary amine groups remain relatively mobile and unhindered during gelation.

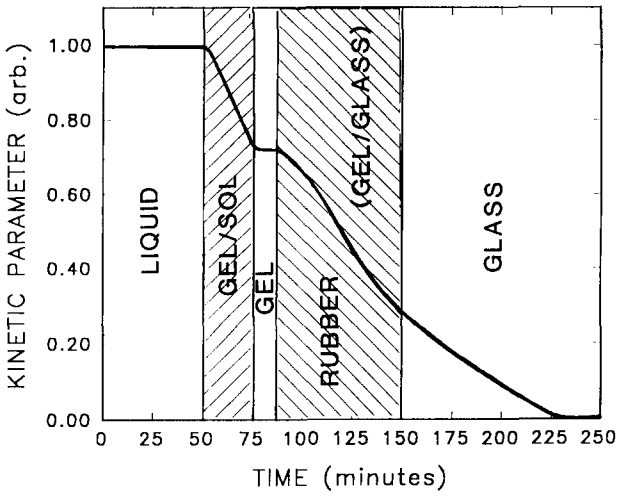

Figure 11 Schematic diagram of changes in kinetic parameter k for the secondary amine–epoxy reaction *versus* cure time at 160°C

The secondary amine–epoxy reaction on the other hand reflects all the rheological changes occurring during cure, as discussed in the light of the d.m.a. results. To obtain a better picture of the changes occurring one can ignore the reactant concentrations and study the changes in the kinetic parameter normally referred to as the rate constant. This requires the assumption that the reaction mechanism stays essentially unchanged throughout the cure. *Figure 11* shows a representation of the kinetic parameter for the secondary amine–epoxy reaction *versus* cure time composed from the main features of the rate curve (*Figure 6*). TGDDM/DDS is seen to pass through five different morphological states during cure at 160°C, two of which are transitory.

Initially the resin is in a liquid state and the kinetic parameter is indeed a constant. At the onset of gelation, where the viscosity increases rapidly, the reactivity of secondary amine towards epoxy drops sharply, stabilizing as the remaining sol fraction is incorporated into the gel. The reactivity is then constant with the resin fully gelled, though this is only for a short time as the crosslinking reaction quickly increases the network structure and vitrification sets in. This is the point seen as a tan δ peak in the d.m.a. study (*Figure 7*) representing the start of the 'freezing out' of backbone chain movements as the number of crosslinks along the chains increase.

As the resin vitrifies the secondary amine reactivity decreases which in turn slows down the vitrification process. Thus at 160°C it takes some 60 min for the resin to totally vitrify and G' to reach a constant value. One might expect the reactivity to be zero in the glassy state, however, it is seen that secondary amine groups continue to react in the glassy TGDDM/DDS at 160°C. The reactivity nonetheless continues to diminish, as the network structure increases, till it is totally extinguished.

It is important to remember that the etherification reactions are occurring simultaneously with the amine reactions and are dominant in the glassy region. The rate curve for etherification (*Figure 8*) is little changed due to gelation though otherwise shows similar features to that for the secondary amine–epoxy reaction with the etherification continuing more strongly in the glassy state. This may be due to the ease of the intramolecular reactions as previously discussed.

The depth of knowledge of the cure of TGDDM/DDS shown to be accessible using near i.r. spectroscopy is ultimately of value in modelling studies of the cure and resulting structure. A previous attempt by Chaio[9] to model the cure of TGDDM/DDS resins using numerical analysis of reaction kinetics was limited by the empirical data and mechanistic knowledge available at the time. Recently, Gupta and Macosko[27] described a modelling approach for the amine–epoxy reaction with etherification using combined statistical and kinetic techniques to predict gel points and cure behaviour. Having kinetic data over the entire cure for the different reactions and knowing chemo-rheological effects will greatly advance such studies[8].

CONCLUSIONS

The concentrations of epoxy, hydroxyl, ether and primary, secondary and tertiary amine groups during the cure of a TGDDM/DDS resin at 160°C have been calculated using near i.r. spectroscopic data. The application of such functional group data to evaluating kinetic parameters and reaction mechanisms has been described and reveals a level of information previously inaccessible for epoxy–amine systems over the entire cure.

The epoxide reaction with both primary and secondary amines was found to be autocatalytic, being catalysed by the hydroxyl groups produced in the epoxy–amine reaction. The secondary amine–epoxy reaction showed a marked substitution effect with k_2/k_1 being 0.215 and was seen to be greatly affected by changes in the rheological properties of the resin during cure. Dynamic mechanical analysis shows that the noticeable changes in rate observed occur at gelation and during vitrification. Two mechanisms are observed for the epoxy–hydroxyl reaction with one being a direct second-order reaction and the other involving catalysis by the tertiary amine groups produced by the secondary amine–epoxy reaction. The sensitivity of the method used to assess mechanistic details is highlighted in a proposed additional reaction of chlorohydrin impurities present in the commercial resin MY721 based on the kinetic data which is supported by mid i.r. spectral analysis of reaction products.

This paper has been concerned with the description of the analytical and numerical methods developed to derive the functional group concentration and empirical reaction rate data. Such an approach can be used to describe the kinetics and mechanisms of cure reactions for not only TGDDM/DDS resins, but also other epoxy–amine systems that lend themselves to study by near i.r. spectroscopy.

ACKNOWLEDGEMENTS

The authors gratefully acknowledge the assistance of Mr Peter Cole-Clarke in providing the LC purified TGDDM and Dr Wayne Garrett whose mathematics program SIMOPR was used in this work. Financial support was provided by a Special Project Grant from the University of Queensland.

REFERENCES

1 Morgan, R. J. and Mones, E. T. *J. Appl. Polym. Sci.* 1987, **33**, 999
2 Mijovic, J., Kim, J. and Slaby, J. *J. Appl. Polym. Sci.* 1984, **29**, 1449
3 Apicella, A., Nicolais, M. I. and Passerini, P. *J. Appl. Polym. Sci.* 1984, **29**, 2083

4 Barton, J. M. *Adv. Polym. Sci.* 1985, **72**, 111
5 Buist, G. J., Hagger, A. G., Houslin, B. J., Jones, J. R., Parker, M. J., Barton, J. M. and Wright, W. W. *Polym. Commun.* 1990, **31**, 265
6 Hagnauer, G. L., Pearce, P. J., Laliberte, B. R. and Roylance, M. E. *ACS Symp. Ser.* 1983, **227**, 25
7 Grenier-Loustolot, M. and Grenier, P. *Br. Polym. J.* 1990, **22**, 303
8 Mertzel, E. A., Perchak, D. R., Ritchey, W. M. and Koenig, J. L. *Ind. Eng. Chem. Res.* 1988, **27**, 586
9 Chaio, L. *Macromolecules* 1990, **23**, 1286
10 Attias, A. J., Bloch, B. and Laupretre, F. *J. Polym. Sci. A* 1990, **28**, 3445
11 George, G. A., Cole-Clarke, P. A., St John, N. A. and Friend, G. *J. Appl. Polym. Sci.* 1991, **42**, 643
12 Luck, W. A. P. and Ditter, W. J. *J. Mol. Structure* 1967–68, **1**, 261
13 Crissler, R. O. and Burrill, A. M. *Anal. Chem.* 1959, **31**, 2055
14 Goddu, R. F. and Delker, D. A. *Anal. Chem.* 1958, **30**, 2013
15 James, D. I., Maddams, W. F. and Tooke, P. B. *Appl. Spectr.* 1987, **41**, 1362
16 George, G. A., Cole-Clarke, P. A. and St John, N. A. *Materials Forum* 1990, **14**, 203
17 Aronhime, M. T. and Gillham, J. K. *Adv. Polym. Sci.* 1986, **78**, 81
18 Cole, K. C., Hechler, J. J. and Noel, D. *Macromolecules* 1991, **24**, 3098
19 Podzimek, S., Dobas, I., Sveska, S., Horalek, J., Tkaczyk, M. and Kubin, M. *J. Appl. Polym. Sci.* 1990, **41**, 1161
20 Williams, D. H. and Fleming, I. 'Spectroscopic Methods in Organic Chemistry', 3rd Edn, McGraw-Hill, London, 1980, pp. 36–73
21 Davies, W. and Savige, W. E. *J. Chem. Soc.* 1950, 181
22 Podzimek, S., Dobas, J., Svestka, S., Eichler, J. and Kubin, M. *J. Appl. Polym. Sci.* 1991, **42**, 791
23 Rozenberg, B. A. *Adv. Polym. Sci.* 1986, **75**, 113
24 Apicella, A. and Nicolais, L. *Adv. Polym. Sci.* 1985, **72**, 69
25 Morrison, R. T. and Boyd, R. N. 'Organic Chemistry', 3rd Edn, Allyn and Bacon, Boston, 1973, pp. 552–578
26 Grenier-Loustalot, M., Metras, F., Grenier, P., Chenard, J. and Horny, P. *Eur. Polym. J.* 1990, **26**, 83
27 Gupta, A. M. and Macosko, C. W. *J. Polym. Sci., Polym. Chem. Edn.* 1990, **28**, 2585